Breaking atomic bonds through vibrational mode localization

Sergey V. Dmitriev[1,2,a], Ju Li[3,b], Nobuhiro Yoshikawa[1,c],

Yoshihisa Tanaka[2,d], Yutaka Kagawa[1,e],

Takayuki Kitamura[4,f] and Sidney Yip[5,g]

[1]Institute of Industrial Science, the University of Tokyo,
Meguro-ku, 4-6-1 Komaba, 153-8505 Tokyo, Japan

[2] National Institute of Materials Science,
1-2-1, Sengen, Tsukuba, Ibaraki, 305-0047, Japan

[3]Department of Materials Science and Engineering, Ohio State University,
Columbus, OH 43210, USA

[4]Department of Engineering Physics and Mechanics, Kyoto University,
Yoshidahonmachi, Sakyoku, Kyoto, Japan

[5]Massachussetts Institute of Technology, 77 Mass. Ave., Cambridge, MA 2139, USA

[a]sergey@iis.u-tokyo.ac.jp, [b]lij@matsceng.eng.ohio-state.edu, [c]yoshi@telu.iis.u-tokyo.ac.jp,
[d]tanaka.yoshihisa@nims.go.jp, [e]kagawa@iis.u-tokyo.ac.jp, [f]kitamura@kues.kyoto-u.ac.jp,
[g]syip@mit.edu

Keywords: Lattice instability, single crystal, surface nucleation, nano-notch, dislocation emission

Abstract. We apply the lattice instability analysis to homogeneously strained single crystal with a flat or defected surface to demonstrate that, in the process of emission of dislocation by an unstable surface, prior to the breaking of atomic bonds, a vibrational mode localizes, foretelling the location and the manner of the impending microscopic catastrophic event.

1. Introduction

Theoretical strength of crystals is one of the classic problems in materials science. Frenkel's formula of theoretical strength reveals the importance of defects in governing the mechanical properties of materials, and it was believed for many decades that theoretical strength is unimportant technologically since we are usually dealing with defected, not ideal, materials. The nucleation and migration of defects can be aided by thermal fluctuations [1,2], a factor not considered in simple "brute-force" strength estimates. However, the importance of theoretical strength is becoming more widely appreciated as technology enters the nano-scale. Materials with small dimensions, e.g., whiskers and carbon nano-tubes, show strengths approaching their theoretical limits. Properties of nano-scale systems, for example, the hardness of epitaxial thin films measured by nano-indentation, can be closer to the properties of ideal single-crystals and differ considerably from the macroscale properties of that material.

It also has been long recognized by theoreticians that a connection exists paradoxically between defect behavior and theoretical strength. Defects like the dislocation core and crack tip provide the necessary leverage to amplify an external shear or tensile stress to the level that can break bonds locally, albeit in an inhomogeneous and asynchronous fashion. Theoretical strength calculations therefore lend zeroth-order insights [3] into how bonds break in defect cores. Analytic theories based on the so-called "equivalent crystal" concept, such as the Peierls-Nabarro model of dislocation core [4,5], cohesive zone model of crack tip [6] and ductility measure based on

nucleation activation energies [7] all have deep inherent connections with theoretical strength concepts [3], and work best when the defect cores are spread-out.

Before considering how bonds break in defect cores, however, it behooves us to understand the detailed process by which bonds break in a perfect crystal during homogeneous defect nucleation, after the bulk theoretical strength has been approached. It is proper to consider the low-temperature limit first. Near T=0, the phonons constitute a complete normal basis for all atomic motions, so any bulk-initiated instability at T=0 must be first triggered by phonon instability. Therefore the theoretical strength of a crystal at T=0 is governed by the requirement that all phonon modes have real frequencies [8]. However, since the energy carried by any individual phonon mode is dispersed/delocalized in the system, in order to create a high-energy defect somewhere, this linear phonon instability must be followed by a *strain localization* process, during which nonlinearity must be involved. For simple crystals where the triggering soft mode is a long wavelength elastic wave, a four-stage defect creation process [9,10] has been proposed and verified by explicit molecular dynamics simulations.

For small-scale systems, surfaces and interfaces are obviously important. Aside from a few recent works [11-13], the theoretical strength of surfaces and interfaces is a totally unexplored area. The dynamical processes of surface-initiated defect nucleation, triggered by soft surface phonon and followed by strain localization of the surface atoms, have not been studied. In the present paper we analyze a 2D model of a crystal with surfaces of different orientations. They can have regular periodic structures, or can embed a defect (e.g., step), and in our case it is a nano-notch. The 2D model was chosen because it serves our purpose of trying to understand the fundamental dynamics very nicely, being rich enough and, at the same time, simple enough to illustrate the contrast between local and global instabilities, and pre- and post-critical strain localization effects.

2. Simulation Details

An important class of lattice instability is crystals having surfaces or interfaces and no other defects (see, e.g. [11-13]). In this situation the translational symmetry is preserved in one (for a fiber) or two (for a film) directions and the discrete Fourier transform can be effectively applied to reduce the number of degrees of freedom in the stability analysis. For 2D fiber and half-space (see Fig. 1(a),(b)) translational symmetry is preserved in x-direction and the small-amplitude vibrational modes are

$$\mathbf{U}(t) = \mathbf{U}^0 \exp[i(k_x l - \omega t)], \qquad (1)$$

where i is imaginary unit; k_x is the vector in reciprocal space; l is an integer specifying a periodic cell; ω is the eigen-frequency of a particular phonon; $\mathbf{U}^0$ is the corresponding eigen-vector containing the components of displacements of all atoms in a periodic cell. Note that the bulk instability of a 2D crystal under homogeneous strain has been analysed in therms of linear phonon modes (P-criterion) in [14].

When spatial periodicity is absent, for example, for the surface with a step or notch, local instability can be studied by assuming that the instability mode is localized near the defect. Atoms around the defect are assumed to be movable while the faraway atoms are fixed at their equilibrium positions (see Fig. 1(c)). Small-amplitude vibrational modes in this case can be expressed as

$$\mathbf{U}(t) = \mathbf{U}^0 \exp(-i\omega t), \qquad (2)$$

where ω is the eigen-frequency of a particular mode and $\mathbf{U}^0$ is the corresponding eigen-vector containing the components of displacements of all movable atoms. This approach is equivalent to that formulated in [11].

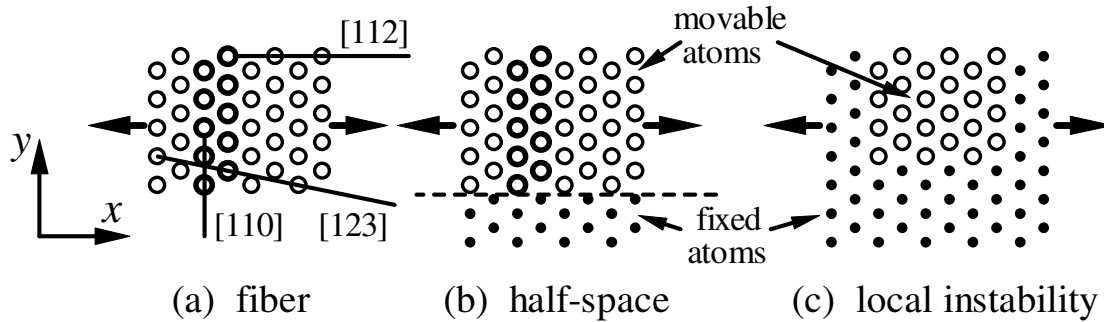(a) fiber   (b) half-space   (c) local instability

Fig. 1. 2D instability problems: (a) fiber, (b) half-space, (c) embedded-region local instability. Instability problems presented in (a) and (b) have translational symmetry along x-direction and are simplified by the discrete Fourier transform. Atoms in a periodic cell are shown by bold open circles. In (b) and (c), movable atoms (open circles) interact with the homogeneously strained continuations of the lattice (dots) which are considered to be fixed when formulating the eigen-problem for the small-amplitude vibrations. Samples are subjected to uniaxial tension or compression along the x-direction, and the surface, which is also parallel to the x-direction, is free of external loads. The case of surface parallel to the [112] crystallographic orientation (2D triangular lattice is regarded here as a (111) plane of fcc crystal) is shown in this figure, but we also study the [110] and [123] orientations as indicated in (a).

Substituting Eq. 1 or Eq. 2 into the linearized equations of motion of the atoms gives an eigenvalue problem with $M \times M$ symmetric matrix where M is the number of degrees of freedom in $\mathbf{U}^0$. For the bulk crystal the approach usually can be applied without any complications because the number of atoms in a primitive cell is usually not large. However, for a film or a fiber, the number of degrees of freedom in a periodic cell depends not only on the crystal structure but also on the thickness of the sample and surface orientation. To reduce the number of degrees of freedom one can concentrate on local instabilities [15,16] near the surface. If a structural instability is initiated at the surface, the corresponding instability mode should be localized near the surface, i.e., the displacements of atoms of the unstable eigenmode should decrease rapidly with the distance from the surface. In this situation, in Eq. 1, one can set the displacements of atoms far from surface equal to zero thus reducing the number of degrees of freedom in the secular equation. When applying this assumption we exclude the global instabilities from consideration. Special care should be taken when global instability modes can be responsible for the instability of the sample, e.g., buckling of rather long and thin fiber under compression [13].

The two-dimensional triangular lattice with lattice parameter a is generated by the vectors $\mathbf{p}_0 = a(1,0)$ and $\mathbf{q}_0 = a(1/2, \sqrt{3}/2)$. In the lattice strained homogeneously with strain components $\varepsilon_{xx}, \varepsilon_{yy}, \varepsilon_{xy}$, the (i,j)th atom has the position vector $\mathbf{r}_{ij} = i\mathbf{p} + j\mathbf{q}$ where $\mathbf{p} = \mathbf{p}_0 + \mathbf{p}_0\mathbf{H}$, $\mathbf{q} = \mathbf{q}_0 + \mathbf{q}_0\mathbf{H}$, and the matrix $\mathbf{H}$ has coefficients $h_{11} = \varepsilon_{xx}$, $h_{12} = h_{21} = \varepsilon_{xy}/2$, $h_{22} = \varepsilon_{yy}$.

We employ the short-range pairwise interatomic potential similar to that used in [8]:

$$\varphi(r) = \begin{cases} \left[\left(\dfrac{r - R_c}{R_a - R_c}\right)^8 - 2\left(\dfrac{r - R_c}{R_a - R_c}\right)^4\right], & r < R_c \\ 0, & r \geq R_c, \end{cases} \tag{3}$$

where r is the distance between two atoms, R_a is the atom radius and R_c is the cut-off radius. Without the loss in generality we set $R_a = 1$. We set $R_c = 1.3R_a$, i.e., each atom interacts only with the nearest neighbors and thus, lattice parameter is $a = R_a = 1$. The energy unit is chosen in a way that $\varphi(R_a) = -1$. Cohesive energy of the unstrained crystal is equal to $E_0 = -3$ per atom. In our previous work [13] we have also used a long-range Lennard-Jones potential and found that, in our numerical setup, the atomic structure of the surface and the crystallographic orientation of the sample play more important role in controlling the instability mechanism than the actual law of interatomic interactions. The atomic mass is normalized to unity which can always be done by proper choice of the time unit.

Three simulation substeps are carried out. (i) Pre-critical relaxation of atoms in *one periodic cell* of the sample is simulated under stepwise increase of uniaxial strain. (ii) At each strain step, after the relaxation is complete, we solve the eigenvalue problem to determine the eigen-frequencies ω and eigenmodes $\mathbf{U}^0$ of small-amplitude vibrations of atoms near their equilibrium positions. The eigenvalue problem is formulated by substituting Eq. 1 or Eq. 2 into the equations of motion of atoms linearized in the vicinity of their equilibrium positions. The number of eigenmodes is equal to the number of degrees of freedom in the (periodic) cell. Vanishing of the frequency of a mode or modes is the criterion of lattice instability. This is the soft phonon mode criterion which is convenient to call the P-criterion with the mnemonic P standing for "phonon" [14]. (iii) Post-critical dynamics of atoms in a supercell consisting of many periodic cells. This simulation is carried out at a fixed external strain slightly exceeding the critical value. Random perturbations of order of 10^{-3} are introduced in the positions of atoms to excite the fall from the unstable equilibrium.

To characterize the degree of localization of an eigenmode we introduce the following localization parameter,

$$L = \frac{\displaystyle\sum_{n=1}^{N} |\mathbf{u}_n|^2}{\left(\displaystyle\sum_{n=1}^{N} |\mathbf{u}_n|\right)^2}, \tag{4}$$

where $\mathbf{u}_n$ is the displacement vector of nth atom. From its very definition, the fewer atoms the displacements are localized onto, the closer L is to unity. On the other hand, the more homogeneous are the displacements of atoms in an eigenmode, the closer L is to a constant of order of N^{-1}, which tends to zero with increase in the number of atoms, N.

3. Surface instabilities in half-space

Analyses of instabilities in fibers have shown that, except for the tension of [110] fiber having atomically flat surface, the instability modes in all other cases are localized near surface [14]. For such modes one can considerably reduce the number of degrees of freedom noting that the amplitude of vibration of atoms situated far from the surface is negligibly small. Thus we come to the half-space instability problem schematically depicted in Fig. 1(b).

In Fig. 2 we show the low-frequency part of spectra of the half-spaces under compression (upper panels) and tension (lower panels) at the critical strain parameter, for the three different orientations. Corresponding unstable eigenmode displacements are depicted in Fig. 3 and the corresponding MD results showing the initial stages of the post-critical transformations are presented in Fig. 4.

In the half-space problem the vibrational spectra do not have acoustic branches. One can see that only tension along [112], panel (d), results in the mode softening at the origin of the Brillouin zone, $k_x = 0$, while in all other cases mode softening occurs either at the zone boundary, $k_x = \pi$, or inside the first Brillouin zone, as in (a).

Unstable displacement modes of fiber (Fig. 5) and half-space (Fig. 9) are also alike except for the case of tension along [110] presented in (b). The difference in this case is due to the fact that the half-space problem does not permit the global instability mode (vanishing of sound velocity) which is responsible for the instability in fiber.
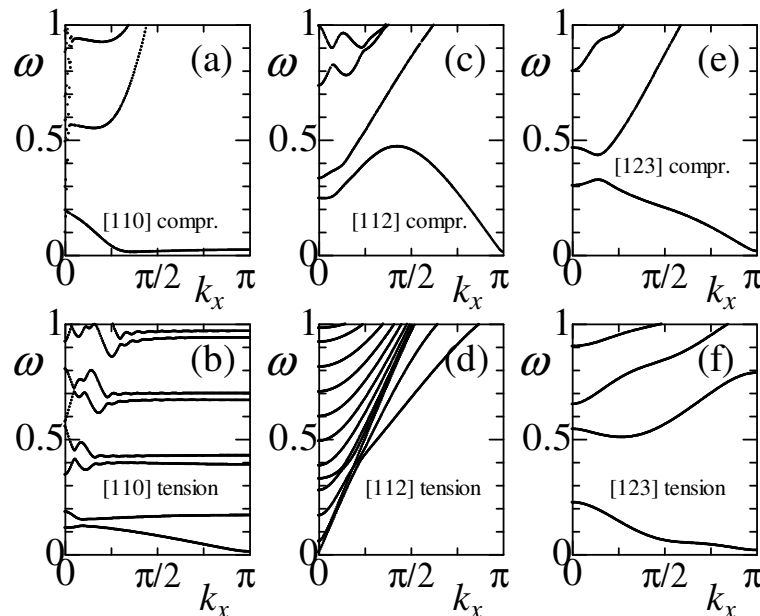

Fig. 2. Low-frequency part of the spectra of half-spaces at critical values of strain. The results are for compression (upper panels) and tension (lower panels) in the direction parallel to the surface for the surface orientations (a),(b) [110], (c),(d) [112], and (e),(f) [123].
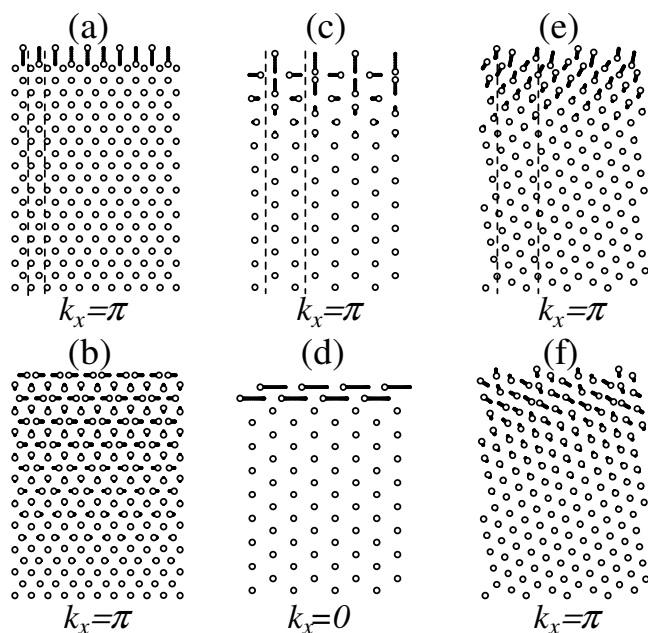
Fig. 3. (a)-(f) Soft eigenmodes corresponding to the instabilities shown in Fig. 2 (a)-(f), respectively. Unstable mode in (b) is not localized at the surface (decrease of the displacement amplitude away from the surface is linear but not exponential) while the other modes are localized and the displacements of atoms reduce very rapidly with the distance from the surface. Only movable atoms are shown. Vertical dashed lines in upper figures show one periodic cell.
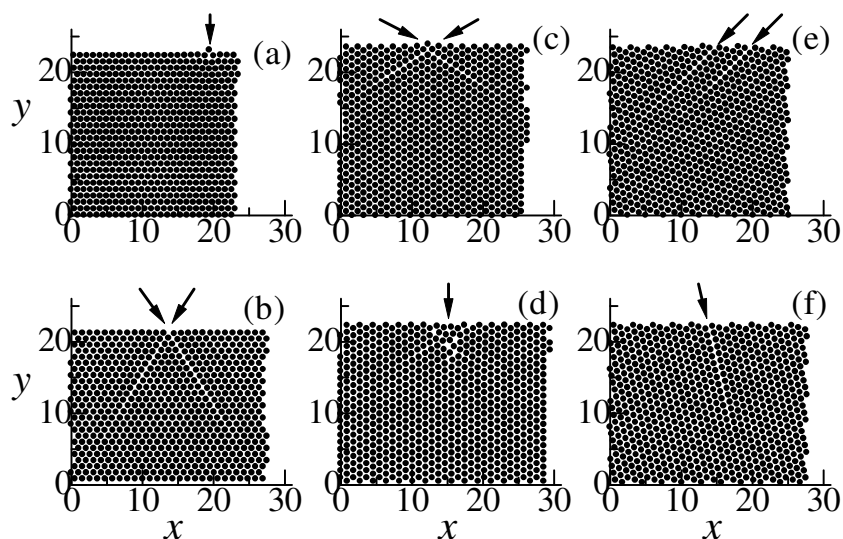

Fig. 4. Initial stage of the post-critical structural transformations simulated by MD. Panels (a)-(f) correspond to the results presented in Fig. 2(a)-(f) and Fig. 3(a)-(f), respectively. In (a), the transformation starts in the single surface monolayer, in (d) it starts from surface reconstruction which affects only two monolayers (cannot be seen here) followed by spinodal decohesion (micro-cracking), and in all other cases the transformation starts from the generation of dislocations at the surface and their gliding in the main slip system.

Critical values of strain for half-space with increase in thickness of movable atom region approach the following values (referred to the corresponding panels of Fig. 2): (a) $\varepsilon^* = -0.0965$, (b) $\varepsilon^* = 0.0583$, (c) $\varepsilon^* = -0.0525$, (d) $\varepsilon^* = 0.0636$, (e) $\varepsilon^* = -0.0493$, (f) $\varepsilon^* = 0.0502$.

MD simulations of the post-critical behavior confirmed the dislocation mechanism of the structural transformations in all cases studied here. However, the dislocations do not appear at the very initial stage of the structural transformations in the cases presented in Fig. 4 (a) and (d). In Fig. 4(a), in accordance with the highly-localized structure of the soft eigenmode presented in Fig. 3(a), the transformation starts in the single surface monolayer. In Fig. 4(d), transformation starts from micro-cracking near the surface. In all other cases one can observe the generation of dislocations at the surface and their gliding in the main slip system.

Localization of unstable modes which can be seen in Fig. 3 can be characterized quantitatively with the use of the localization parameter L given by Eq. 4. The wave vector of the unstable mode is a priori unknown and, generally speaking, parameter L should be analyzed for different k_x. The situation is simplified for the embedded-region local instability problems because here the spatial periodicity is absent. We would like to use this simplification and the quantitative analysis of L will be done in the following sections.

One qualitative remark can be made already here. Crystal with a surface always has spatially localized surface modes even at zero strain. Generally speaking, the displacement pattern in the unstable mode depends on loading conditions, e.g., pure tension or tension in combination with shear and so on, and thus, the unstable localized mode usually does not coincide with the original surface mode.

4. Embedded-region instability

Now we turn to the lattice instability problem in the absence of translational symmetry. This approach can be applied to predict the near-defect local instabilities, e.g., near a kinked step on a surface, near a dislocation in the bulk, near a crack tip, etc. However, here we apply this approach to the analysis of the periodic surface to have a possibility to compare the results with that obtained above. The main idea of using the local instability analysis is to decrease the number of degrees of freedom. Only atoms near the defect are assumed to be movable and they interact with rigid continuation of the strained equilibrium lattice, as it is schematically shown in Fig. 1 (c). Surface plays the role of defect in our case.

Let us consider the [110] surface under tension/compression. In Fig. 5 we show the instability modes for (a) compression and (b) tension parallel to surface. Only movable atoms are shown. In this example, the region with movable atoms consists of $N_x = 20$, $N_y = 16$ monolayers.

The mode in Fig. 5(a) should be compared to that depicted in Fig. 3(a). One can see that this is actually the same mode subjected to clamping boundary conditions, analogous to forming a Gaussian wave pack or wavelet out of plane waves. The similarity of the instability modes ensures good convergence of the critical strain with increase in N_x, N_y to the value obtained for the half-space with rather thick layer of movable atoms. One more reason for the good convergence is the localization of the unstable mode when strain approaches a critical value. This can be seen in Fig. 6, where we show (a) frequencies of the five lowest-frequency modes and (b) the localization parameter, L, defined by Eq. 4, for the lowest-frequency mode as the functions of compressive strain ε_{xx}.

Similar results were obtained for the case of compressive strain. The soft mode obtained in local instability analysis and presented in Fig. 5(b) resembles the staggered instability mode in Fig. 3(b),

observed for half-space. With increase in N_x, N_y, the result of local lattice instability analysis converges to the critical strain value obtained for half-space with sufficiently thick layer of movable atoms. The mode localization in this case is illustrated by Fig. 7.
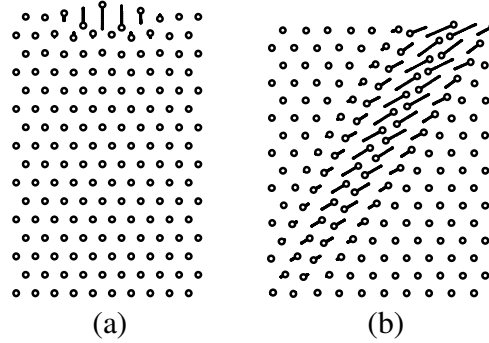

(a)   (b)

Fig. 5. Instability modes in the embedded-region local instability analysis (see Fig. 1 (c)) for [110] surface. Samples in (a) and (b) are under compression and tension parallel to surface, respectively. Only movable atoms are shown. Number of monolayers along x and y directions is equal to $N_x = 20$, $N_y = 16$.
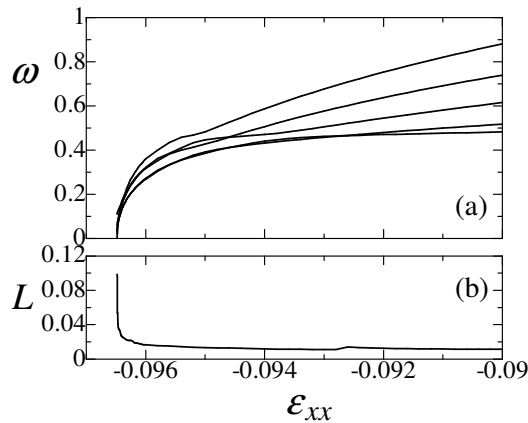

Fig. 6. (a) Frequencies of the five lowest-frequency modes and (b) the localization parameter for the lowest-frequency mode as the functions of homogeneous compressive strain ε_{xx} applied parallel to the [110] surface (see Fig. 5(a)).
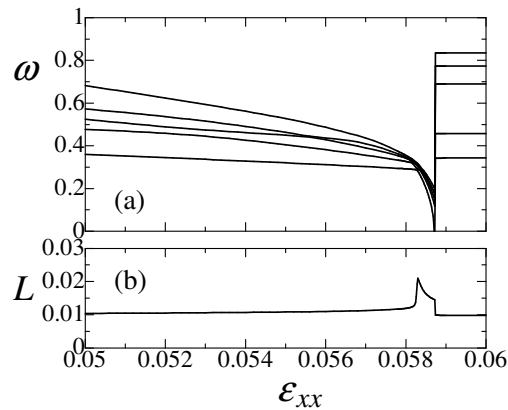

Fig. 7. Same as in Fig. 6 but for tensile strain ε_{xx} (see Fig. 5(b)).

5. Instability at nano-notch

In Fig. 8 and Fig. 9 we present the results of simulation for instability at the [110] surface with a nano-notch. The numerical setup shown in Fig. 1 (c) was used for this study, i.e., a rectangular block of movable atoms around notch is surrounded by the homogeneously strained half-space with fixed atoms to study the local instability near the notch. Tensile strain ε_{xx} is applied parallel to the surface. Notch has closed-packed faces with the angle of $60°$ between them. The depth of notch, D, is measured in the number of monatomic layers, with $D = 0$ meaning atomically flat surface. In Figs. 8 (a)-(e) and in Fig. 9, the results for $D = 1$ are presented.

Left panels in Figs. 8 (a)-(e) show the positions of movable atoms while right panels show the lowest frequency vibrational modes. In Fig. 8 (a) the unstrained relaxed configuration is shown. In (b), $\varepsilon_{xx} = 0.0318$, and in (c), $\varepsilon_{xx} = 0.0336$ the structures at increasing strain are shown, revealing the change in the symmetry of the lowest-frequency mode due to the crossing of the branches of the dispersion curves. In Fig. 8 (d), we have $\varepsilon_{xx} = 0.0347$, which is very close to the critical value. In (e), $\varepsilon_{xx} = 0.035$, the post-critical configuration is shown after one dislocation was emitted and moved to the boundary of the block with movable atoms.

The influence of the nano-notch depth, D, on the critical strain, ε_{xx}^*, is shown in Fig. 8 (f). Note that the decrease in ε_{xx}^* by roughly factor of three (from $\varepsilon_{xx}^* \approx 0.06$ to $\varepsilon_{xx}^* \approx 0.02$) due to increase in D means the one order of magnitude decrease in the critical elastic energy.
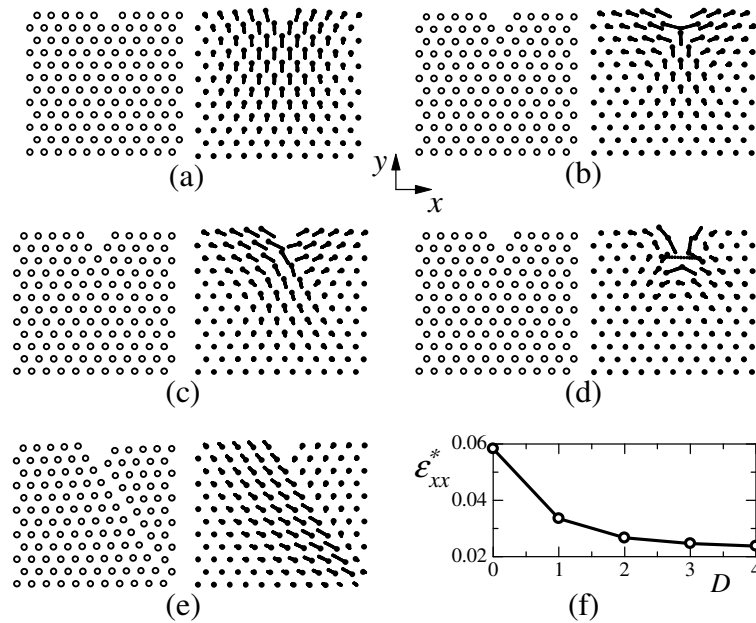

Fig. 8 [110] surface with nano-notch under tension along x-direction. In (a)-(e) left panels show the atomic positions near the nano-notch while right panels show the lowest-frequency eigenmode. Only movable atoms are shown but they interact with the homogeneously strained continuation of the half-space as it is illustrated by Fig. 1(c). Magnitudes of strain are (a) $\varepsilon_{xx} = 0$; (b) $\varepsilon_{xx} = 0.0318$, left arrow in Fig. 9(b); (c) $\varepsilon_{xx} = 0.0336$, middle arrow in Fig. 9(b); (d) $\varepsilon_{xx} = 0.0339$, pre-critical strain with maximum localization parameter, L, not indicated by arrow in Fig. 9(b); (e) $\varepsilon_{xx} = 0.035$, post-critical state, right arrow in Fig. 9(b). In (f), critical strain is shown as the function of notch depth, D, measured in number of monolayers. In (a)-(d) the case of $D = 1$ is presented.
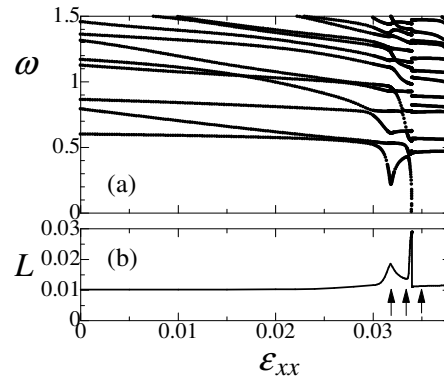
Fig. 9. (a) Low-frequency part of the vibration spectrum of surface with $D=1$ nano-notch (see Fig. 8) and (b) the localization parameter for the lowest-frequency mode as the functions of homogeneous tensile strain ε_{xx} applied parallel to the [110] surface. Discontinuities in the curves correspond to the instability point, $\varepsilon_{xx}=0.0339$, when frequency of a particular phonon mode vanishes and dislocation is emitted by nano-notch. Vanishing of the unstable mode frequency is accompanied by the sharp increase in the localization parameter, L.

Pre-critical localization of the lowest-frequency mode can be visually observed from Fig. 8 by comparison of the pre-critical vibrational mode shown in (d) with the far-from-instability pictures (a)-(c) and the post-critical mode (e). Quantitative result is presented in Fig. 9, where we show (a) the low-frequency part of the vibrational spectrum of surface with $D=1$ nano-notch and (b) the localization parameter, L, defined by Eq. 4, for the lowest-frequency mode as the functions of strain ε_{xx}. Discontinuities in the curves correspond to the instability point, $\varepsilon_{xx}=0.0339$, when frequency of a particular phonon mode vanishes and dislocation is emitted by nano-notch. Vanishing of the unstable mode frequency is accompanied by sharp increase in the localization parameter, L.

6. Discussion and conclusions

The role of surface in the lattice instability problem has been studied numerically for 2D crystal model. It has been demonstrated that, in many cases, the problem can be simplified by considerable reduction of number of degrees of freedom involved in the analysis. This is achieved by substituting the eigenvalue problem formulated for the whole sample with the problem dealing with local instabilities. Such substitution is justified by the fact that usually, prior to the atomic bond breaking, spatial localization of an unstable mode does take place.

Defected crystals always have vibrational modes localized near defects. However, the displacement pattern in the unstable mode of critically loaded crystal depends on loading conditions and thus, the unstable localized mode usually does not coincide with the original localized mode.

The influence of surfaces orientation has been studied. We always applied homogeneous tension/compression parallel to surface and thus, changing the crystallographic orientation of the sample, we changed not only the structure of the surface but also the orientation of the slip systems with respect to the loading axis (Schmidt factor). Particularly we have studied surfaces having [110], [112], and [123] crystallographic orientations (2D triangular lattice is considered here as a (111) plane of fcc crystal) with [110] surface being atomically flat, [112] surface being rough, and [123] surface being quasi-vicinal. Only in the case of tension of half-space with [110] surface the instability with respect to non-localized mode was responsible for the collapse of the system while in all other cases a local near-surface instability preceded global one. Among these cases, only in

tension of [112] surface, local instability was not the catastrophic one and it resulted in a local near-surface atomic reconstruction followed soon by a catastrophic global instability. In all other cases the collapse of the system was observed due to a near-surface local instability mode. Thus, surfaces under compression were always unstable with respect to a local mode and surfaces under tension demonstrated global instabilities for low-index orientations and local instabilities for high-index orientations. This trend also suggests that, in a realistic situation with steps on surface, local instabilities can control the strength of the surface under homogeneous strain.

We have found that the critical strains for near-surface lattice instabilities can be noticeably lower than that in bulk instabilities [14] especially for real surfaces with steps or nano-scratches.

Temperature effect, 2D lattices with complex structures, realistic 3D crystals are among the topics for future studies on the role of various defects in lattice instability.

References

[1] T. Zhu, J. Li and S. Yip: Phys. Rev. Lett. Vol. 93 (2004), p. 025503.
[2] T. Zhu, J. Li and S. Yip: Phys. Rev. Lett. (2004), accepted.
[3] S. Ogata, J. Li, N. Hirosaki, Y. Shibutani and S. Yip: Phys. Rev. B Vol. 70 (2004), p. 104104.
[4] R. Peierls: Proc. Phys. Soc. London Vol. 52 (1940), p. 34.
[5] F.R.N. Nabarro: Proc. Phys. Soc. London Vol. 59 (1947), p. 256.
[6] M.L. Falk, A. Needleman and J. R. Rice: J. Phys. IV Vol. 11 (2001), p. 43.
[7] J.R. Rice and G.E. Beltz: J. Mech. Phys. Solids Vol. 42 (1994), 333.
[8] K.J. Van Vliet, J. Li, T. Zhu, S. Yip and S. Suresh: Phys. Rev. B Vol. 67 (2003), p. 104105.
[9] J. Li, K.J. Van Vliet, T. Zhu, S. Yip and S. Suresh: Nature Vol. 418 (2002), p. 307.
[10] J. Li, A.H.W. Ngan and P. Gumbsch, Acta Mater. Vol. 51 (2003), p. 5711.
[11] T. Kitamura, Y. Umeno and R. Fushino: Mater. Sci. Eng. A Vol. 379 (2004), p. 229.
[12] T. Kitamura, Y. Umeno and N. Tsuji: Comput. Mater. Sci. Vol. 29 (2004), p. 499.
[13] S.V. Dmitriev, T. Kitamura, J. Li, Y. Umeno, K. Yashiro and N. Yoshikawa: Acta Mater. (submitted).
[14] S.V. Dmitriev, J. Li, N. Yoshikawa and Y. Shibutani: Phil. Mag. (in press).
[15] J. Li and S. Yip: Phys. Rev. B Vol. 56 (1997), 3524.
[16] C.S. Jayanthi, M. Tang, S.Y. Wu, J.A. Cocks and S. Yip: Phys. Rev. Lett. Vol. 79 (1997), p. 4601.